Range-separation parameter in tuned exchange–correlation functionals: successive ionisations and the Fukui function

Jonathan D. Gledhill,[†] Frank De Proft,[‡] and David J. Tozer[*,†]

Department of Chemistry, Durham University, South Road, Durham DH1 3LE, UK, and Eenheid Algemene Chemie (ALGC), Vrije Universiteit Brussel (VUB), Pleinlaan 2, 1050, Brussels, Belgium

E-mail: d.j.tozer@durham.ac.uk

Abstract

The range-separation parameter in tuned, range-separated exchange–correlation functionals is investigated in two contexts. First, the system-dependence of the parameter is investigated for a series of systems obtained by successively ionising a single species, paying particular attention to the degree of linearity in the energy versus electron number curve. The parameter exhibits significant system-dependence and so achieving near-linearity in one segment of the curve leads to strong non-linearity in other segments. This provides a challenging test case for the development of new functionals designed to overcome the known problems of this class of functional. Next, the study considers whether a range-separation parameter tuned to a Koopmans *energy* condition is also applicable for the analogous *density* condition. This is tested by comparing two formulations of the Fukui function of conceptual density functional theory,

[*]To whom correspondence should be addressed
[†]Durham University
[‡]Vrije Universiteit Brussel

for three representative systems. Both formulations yield the same general features and are not highly sensitive to the range-separation parameter. However, the agreement between the two is near-optimal when the energy-tuned parameter is used, indicating that this parameter is applicable for the analogous density condition.

1 Introduction

In recent years, there has been significant interest in the use of range-separated (RS)[1–4] exchange–correlation functionals in Kohn–Sham density functional theory (DFT).[5] These functionals partition the r_{12}^{-1} operator in the exchange term into short- and long-range components, with a range-separation parameter, μ, controlling the rate at which the long-range behaviour is attained. The value of μ can be fixed or it can be 'tuned' on a system-by-system basis by minimising some tuning norm.[6–20] Whether the parameter is fixed or tuned, it is well established that such functionals yield improvements in many long-range properties, most notably charge-transfer excitation energies, and they have become the functional of choice in many studies.

In Ref. 15, we investigated a wide range of norms for use in tuned, range-separated functionals. The norms were largely based on Koopmans conditions, which arise from the piecewise linearity[21] of the exact electronic energy, E, as a function of electron number, N. We assessed the quality of frontier orbital energies, orbital energy differences, ionisation potentials and electron affinities. We also quantified the linearity of the E *vs* N curves and highlighted a fortuitious error cancellation between the failure to reproduce the Koopmans conditions and errors in calculated ionisation potentials and electron affinities.

The key feature of tuned range-separated functionals is that μ is determined on a system-by-system basis. As noted by Karolewski *et al.*[14] this can lead to problems, particularly the violation of size-consistency. It is therefore of interest to quantify the degree of system-dependence of μ; examples of strong system-dependence may provide challenging test cases for the development of new functionals designed to overcome the problems highlighted in

Ref. 14. The first aim of the present study is to consider this system dependence. Rather than considering a series of different atoms and molecules, however, we consider systems obtained by successively ionising a *single species*, paying particular attention to the degree of linearity in the segments of the E *vs* N curve.

The second aim of the study is to consider whether a value of μ determined using a regular energy-based norm is also applicable for the determination of non-energy-based quantities. Specifically, the exact electron density is also piecewise linear[21] in N and so we investigate whether a value of μ tuned to a Koopmans *energy* condition is also applicable for the analogous *density* condition. We test this using the Fukui function,[22–26] which is a key quantity in conceptual DFT.[27]

2 Results

We use a tuned version of the CAM-B3LYP functional,[4] with modified parameters $\alpha = 0$ and $\beta = 1$, meaning the fraction of exact exchange increases from zero to 100%, at a rate controlled by μ. The CADPAC[28] and Gaussian 09[29] programs were used.

2.1 Successive ionisations

First, we consider the variation of μ for successive ionisations of a single species using a standard tuning norm based on the HOMO Koopmans condition. In the context of an E *vs* N curve with fixed external potential v, the HOMO energy of an integer N-electron system is the slope of the curve[30–32] on the electron-deficient side of the integer N,

$$\varepsilon_{\text{HOMO}} = \left(\frac{\partial E}{\partial N}\right)_v^- , \tag{1}$$

where we have assumed that the usual generalised Kohn–Sham approach[33] is used. The piecewise linearity[21] of the exact E *vs* N curve means that the derivative in eq. (1) should be identical to the finite-difference derivative obtained from the N and $N-1$ integer energies,

which is just the negative of the vertical ionisation potential

$$-I = E_N - E_{N-1}\,, \tag{2}$$

and so the tuning norm is

$$H = |\varepsilon_{\text{HOMO}} + I|\,. \tag{3}$$

We perform calculations at a range of μ values and define the optimal value, denoted μ^*, to be the one that minimises H.

The carbon atom is the archetypal system for the study of E *vs* N curves and so we consider the systems from C^- to C^{5+}, containing seven to one electrons, using the aug-cc-pCVTZ basis set. Figure 1 plots the value of $\varepsilon_{\text{HOMO}} + I$ as a function of μ, for each species. In all cases, the value reduces smoothly with increasing μ. The minimum of the absolute value of each curve gives the μ^* values, which are listed in table 1. It is immediately apparent that there is significant variation in μ^* for the different systems. The curves in fig. 1 for C^-, C, C^+ and C^{4+} each cross $H = 0$ at finite, but different values of μ^*. The curves for C^{2+} and C^{5+} merely approach zero as μ tends to infinity, whilst the C^{3+} curve tends asymptotically to a positive value.

Table 1: Optimal parameters, μ^*, obtained by minimising the norm, H.

Species	$\mu^*/{a_0}^{-1}$	
C^-	0.37	
C	0.66	
C^+	1.00	
C^{2+}	∞	$(H \to 0)$
C^{3+}	∞	$(H \to +\text{ve})$
C^{4+}	5.89	
C^{5+}	∞	$(H \to 0)$

Next, E *vs* N curves were generated for each adjacent pair of species. This was achieved by incrementing the occupation of the relevant frontier orbital from zero to one in steps of

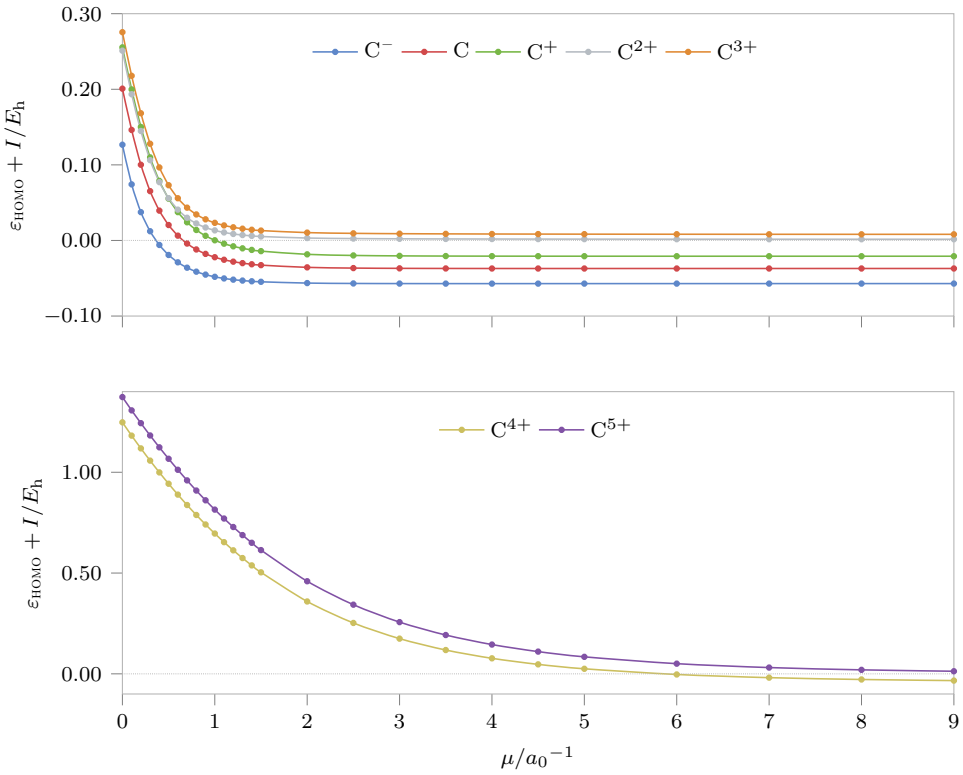

Figure 1: Variation of $\varepsilon_{\mathrm{HOMO}} + I$, as a function of μ.

0.05, and computing the energy at each point with a fixed value of μ. In order to intuitively compare the E *vs* N data for each pair of species on a single plot, and to avoid large differences in scale, we actually consider an E *vs* N *deviation* curve, plotting ΔE against ΔN. ΔE is the difference between the computed energy and the desired behaviour—an interpolated straight line between the integer-N points. ΔN is the fractional occupancy of the relevant frontier orbital, such that the system with smaller integer N is described by $\Delta N = 0$, and the system with larger integer N is $\Delta N = 1$. In this way, the closer a plot is to a straight line along zero, the closer it is to being a linear E *vs* N segment. By construction, the interpolated and calculated energies agree at integer. A horizontal line along zero indicates a linear E *vs* N curve, whilst a positive/negative deviation indicates a concave/convex curve. The first two rows of fig. 2 show the E *vs* N deviation curves for each of the μ^* values in table 1 (we choose $\mu = 1000\,{a_0}^{-1}$ as effectively infinite). Each curve is labelled by the system corresponding to $\Delta N = 1$, with colours consistent with fig. 1.

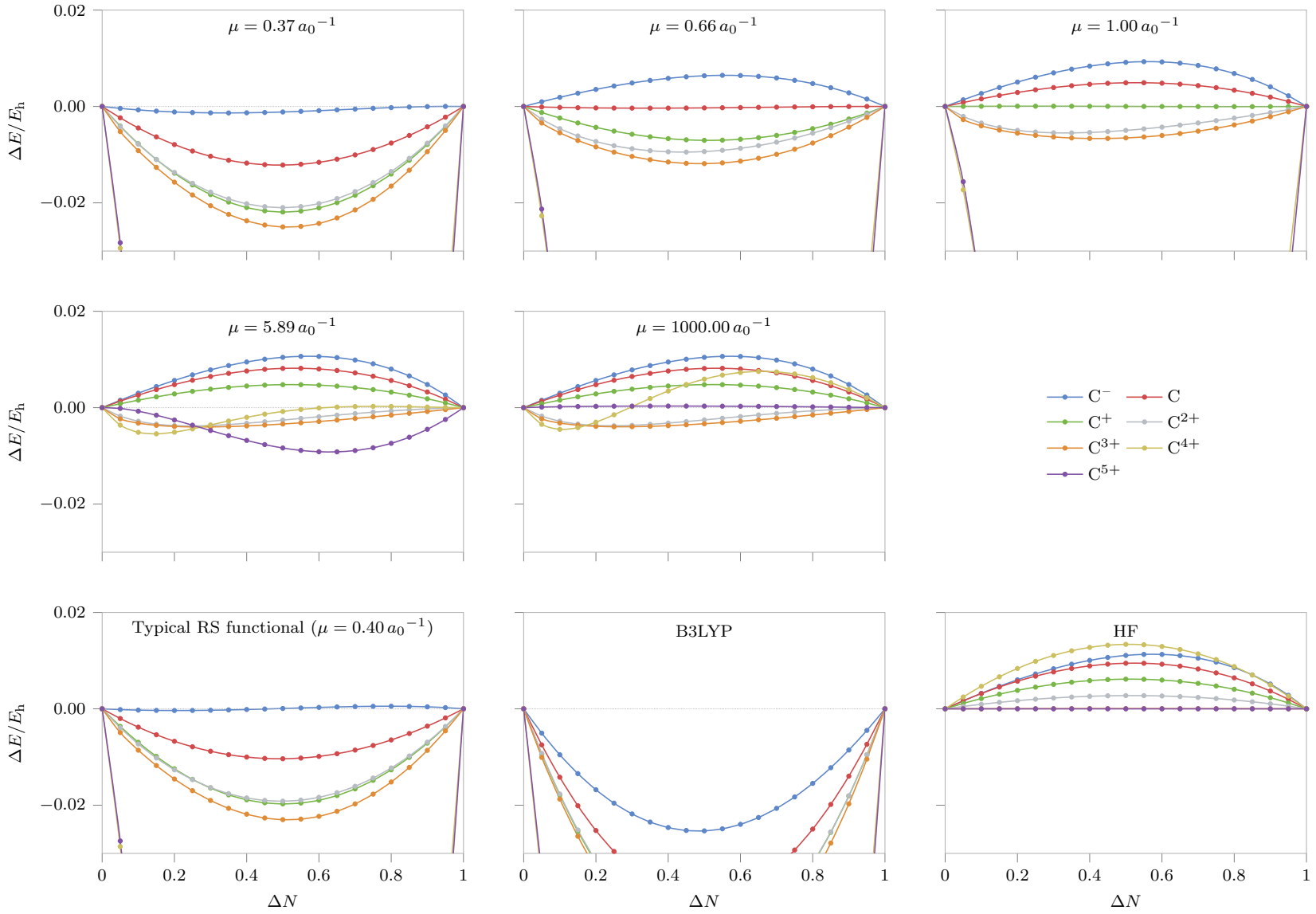

Figure 2: *E vs N* deviation curves for adjacent species using the μ^* values in table 1, together with non-tuned functionals and Hartree-Fock theory. Each curve is labelled by the system corresponding to $\Delta N = 1$.

In the context of fig. 2, the condition $H = 0$ corresponds to a limiting slope of zero, as ΔN approaches unity, and this is clearly reflected in the plots. For C^-, C, C^+ and C^{4+}, where a well-defined, finite μ^* is obtained giving $H = 0$, the limiting slope is zero when $\mu = \mu^*$. For C^{2+} and C^{5+}, where H decays to zero towards infinite μ, the behaviour is approached when computed using very large μ. For C^{3+}, where H decays to a positive asymptote, the behaviour is not observed.

The behaviour of the unconstrained end ($\Delta N = 0$) is less intuitive. If the functional were exact, the slope here would be equal to that at $\Delta N = 1$, and remain constant between $0 < \Delta N < 1$. For several of the systems, this is approximately the case and the curves are near-linear. For others, the curves are more S-shaped.

The plots in fig. 2 illustrate the significant dependence of E *vs* N curves on the precise value of μ, and reinforce previous observations that it is not possible to enforce linearity on two segments of the curve with a single value of μ. This is particularly relevant for the calculation of fundamental gaps, which involves slopes in adjacent segments.

For reference, the final row of fig. 2 presents E *vs* N deviation curves determined using a typical, fixed-μ, range-separated functional ($\mu = 0.40\, {a_0}^{-1}$), together with the conventional B3LYP functional[34–38] and Hartree-Fock theory. The curves from the typical range-separated functional are, of course, very similar to those from $\mu = 0.37\, {a_0}^{-1}$, and they are a notable improvement over those from B3LYP, which are highly convex. The Hartree-Fock curves are concave, except for the curve labelled C^{5+}, which is exactly horizontal because the electron number varies between zero and one and so Hartree-Fock theory is exact. We note that the functional with $\mu = 1000\, {a_0}^{-1}$ is effectively equivalent to using the Hartree–Fock functional with correlation added. The difference between the $\mu = 1000\, {a_0}^{-1}$ and Hartree-Fock curves can therefore be traced to the correlation functional.

We make one final comment. The quantity H involves the calculated I, rather than the experimental value, I^0. Hence, enforcing $H = 0$ will only satisfy the exact condition $\varepsilon_{\text{HOMO}} = -I^0$ if the additional condition, $I = I^0$, is also satisfied. In our previous work,

we highlighted a convenient cancellation of errors between the failure to satisfy $H = 0$ and $I = I^0$. It is therefore pertinent to ask which values of μ yield I values closest to I^0. Results are presented in table 2. Consistent with our earlier work, the values are not the same as the values in table 1, facilitating possible error cancellations.

Table 2: Optimal parameters, μ^*, obtained by minimising the difference between I and I^0.

Species	$\mu^*/{a_0}^{-1}$
C^-	0.61
C	∞
C^+	0.12
C^{2+}	0.61
C^{3+}	3.0
C^{4+}	0.06 or 2.71
C^{5+}	5.80

2.2 Extension to electron densities: the Fukui function

Next, we consider the extension to the electron density in the context of the Fukui function, defined as the first derivative of the electron density with respect to N, at fixed external potential,

$$f(\boldsymbol{r}) = \left(\frac{\partial\rho(\boldsymbol{r})}{\partial N}\right)_v . \tag{4}$$

Specifically, we consider the Fukui function evaluated on the electron-deficient side of the integer N,

$$f^-_{\text{deriv}}(\boldsymbol{r}) = \left(\frac{\partial\rho(\boldsymbol{r})}{\partial N}\right)^-_{v(\boldsymbol{r})} . \tag{5}$$

where we have added the subscript 'deriv' to emphasise that the quantity is explicitly evaluated as a derivative. This Fukui function corresponds to a generalisation[22,23] of Fukui's frontier molecular orbital reactivity index,[24–26] measuring the reactivity of a site towards electrophilic attack, provoking the loss of an electron. The piecewise linearity[21] of the exact electron density with N means that the derivative in eq. (5) should be identical to the

finite-difference (FD) value determined from densities of integer systems,

$$f^-_{\mathrm{FD}}(\boldsymbol{r}) = \rho_N(\boldsymbol{r}) - \rho_{N-1}(\boldsymbol{r}) \tag{6}$$

There is therefore a direct analogy between the equivalence of eqs. (5) and (6), which involve the electron density, and the equivalence of eqs. (1) and (2), which involve the electronic energy. Given that the μ^* obtained by minimisation of the norm H in eq. (3) maximises the agreement between the energy quantities in eqs. (1) and (2), it is natural to investigate the extent to which it also maximises the agreement between the Fukui functions in eqs. (5) and (6).

We therefore need to compare the Fukui function calculated in two ways. The FD expression in eq. (6) is easily evaluated by calculations on integer systems. For eq. (5), we use the numerical approximation

$$f^-_{\mathrm{deriv}}(\boldsymbol{r}) = \frac{\rho_N(\boldsymbol{r}) - \rho_{N-0.01}(\boldsymbol{r})}{0.01} \tag{7}$$

involving calculations on integer and fractional electron number systems. We note that Yang *et al.*[39] recently presented the theory for the analytic evaluation of this derivative. See Refs. 40–42 for related studies.

Following Yang *et al.*,[39] we consider the Fukui functions in the He and Be atoms, together with the H_2CO molecule, using the cc-pVQZ basis set. We plot the Fukui functions in eqs. (6) and (7), together with their difference

$$\Delta f^-(\boldsymbol{r}) = f^-_{\mathrm{deriv}}(\boldsymbol{r}) - f^-_{\mathrm{FD}}(\boldsymbol{r})\,. \tag{8}$$

For the atoms, all three quantities are spherically symmetric and are plotted along the radial coordinate, r. For H_2CO, the quantities are plotted along the principal axis, z, containing the C=O bond. The values of μ^* were calculated to be 1.09, 0.82, and $0.46\,{a_0}^{-1}$ for He, Be,

and H_2CO, respectively.

Figure 3 plots $f_{\text{FD}}^{-}(\boldsymbol{r})$ and $f_{\text{deriv}}^{-}(\boldsymbol{r})$ for the He atom for selected values of μ. We consider $\mu = \mu^*$, which is the value obtained by minimising H. For comparison, we also consider $\mu = 0\,{a_0}^{-1}$, which is a generalised gradient approximation (GGA) functional, and $\mu = 0.40\,{a_0}^{-1}$, which again represents a typical fixed-μ, range-separated functional. On the scale plotted, the $f_{\text{FD}}^{-}(\boldsymbol{r})$ Fukui functions for the different μ values are essentially indistinguishable, whereas differences between the $f_{\text{deriv}}^{-}(\boldsymbol{r})$ functions are evident. This is similar to the analogous energy quantities, where ionisation potentials computed from integer energies are generally less sensitive to μ, than HOMO energies are. Figure 4 plots the differences between the two Fukui functions. The agreement between the functions is notably better when $\mu = \mu^*$, than when $\mu = 0\,{a_0}^{-1}$ (GGA) or $\mu = 0.40\,{a_0}^{-1}$ (range-separated).

Figures 5 and 6 present plots for the Be atom where analogous results are obtained. The improved agreement when $\mu = \mu^*$ is particularly pronounced in the valence region of fig. 6.

Finally, figs. 7 and 8 present results for the H_2CO molecule. Although the extent to which the two Fukui functions agree in fig. 8 depends on the precise choice of spatial region, the agreement is generally better with $\mu = \mu^*$ than with $\mu = 0\,{a_0}^{-1}$ (GGA). The agreement is similar for $\mu = \mu^*$ and $\mu = 0.40\,{a_0}^{-1}$ (range-separated) due to the similar μ values. The trends indicate that whilst the agreement in some regions of space would improve by further increasing μ, it would degrade in other regions.

Overall, for these representative systems, the Fukui functions $f_{\text{FD}}^{-}(\boldsymbol{r})$ and $f_{\text{deriv}}^{-}(\boldsymbol{r})$ exhibit the same general features and are not highly sensitive to the choice of μ. However, the agreement between the two functions is indeed near-optimal when $\mu = \mu^*$, indicating that this energy-tuned parameter is applicable for the analogous density condition.

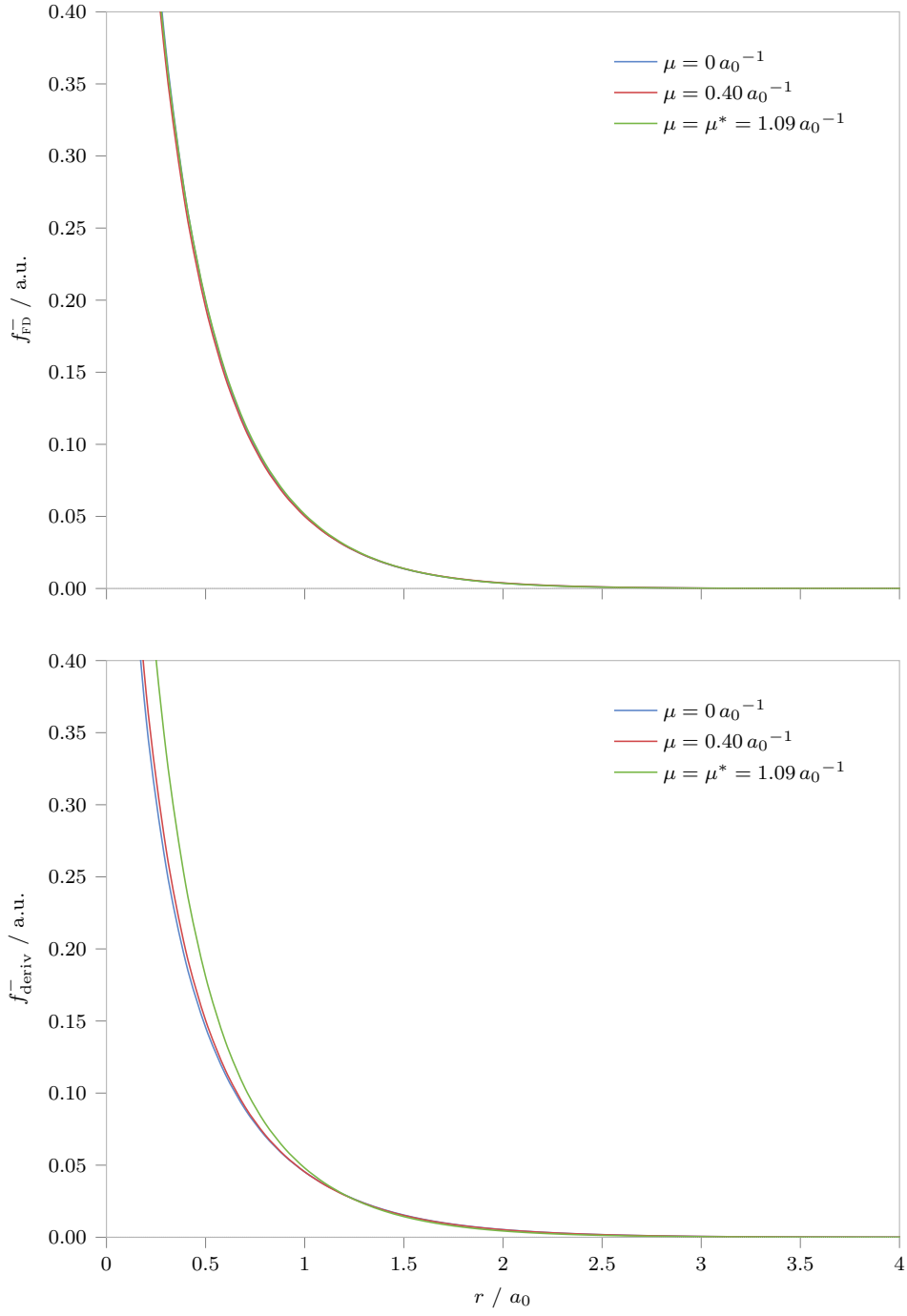

Figure 3: Fukui functions for the He atom

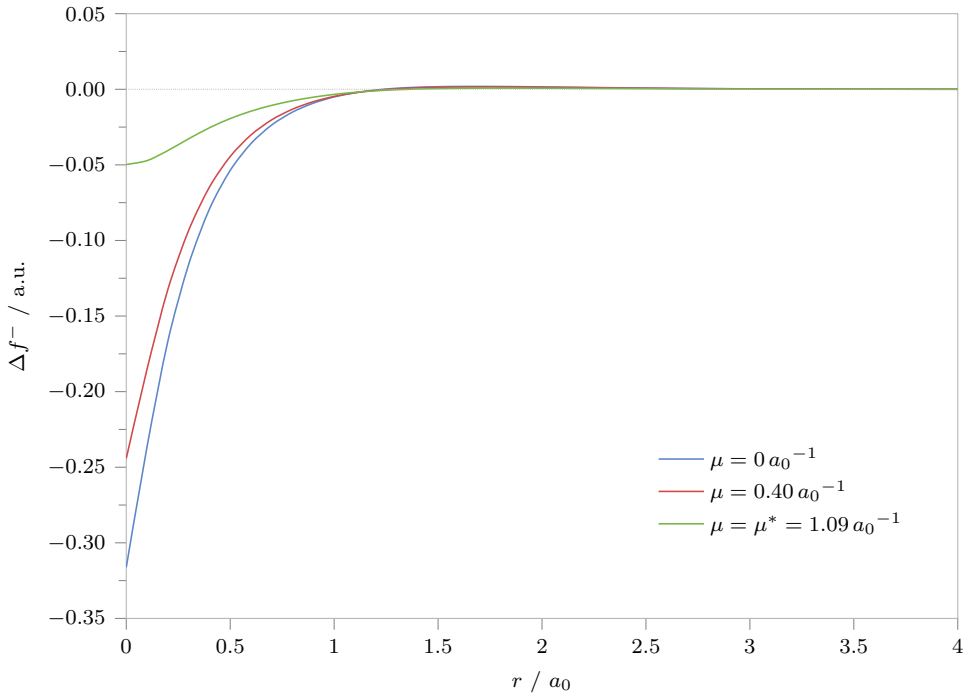

Figure 4: Fukui function differences for the He atom

3 Conclusions

The parameter μ is a key feature in tuned, range-separated exchange–correlation functionals and we have investigated the system-dependence and transferability of this parameter. For C^- to C^{5+}, the optimal μ values differ significantly and so achieving near-linearity in one segment of an E *vs* N curve leads to strong non-linearity in other segments. This provides a challenging test case for the development of new functionals designed to overcome the deficiencies highlighted in Ref. 14. For the Fukui functions of three representative systems, both formulations yield the same general features and the results are not highly sensitive to μ. However, the agreement between the two is near-optimal when $\mu = \mu^*$, indicating that this energy-tuned parameter is applicable for the analogous density condition.

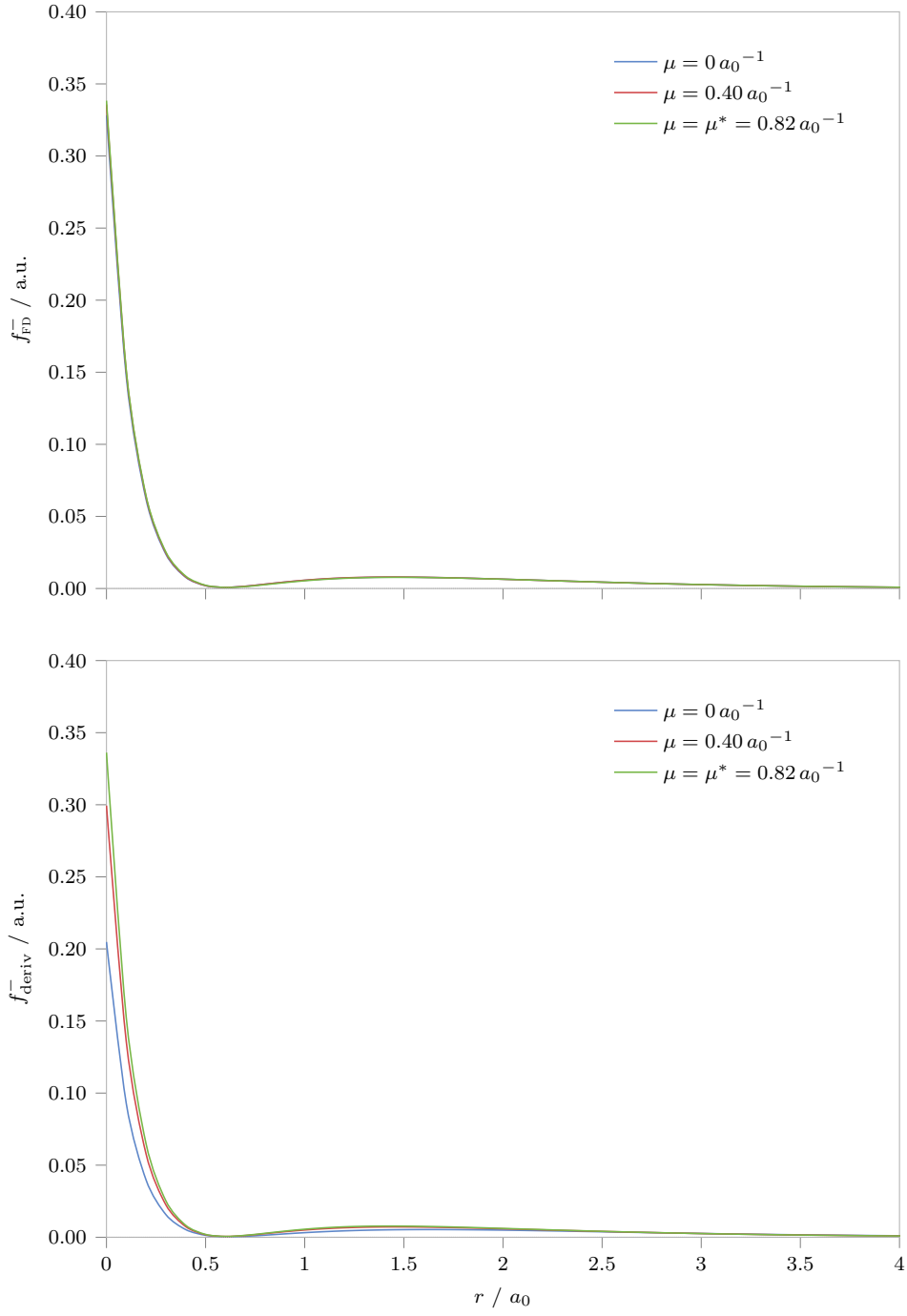

Figure 5: Fukui functions for the Be atom

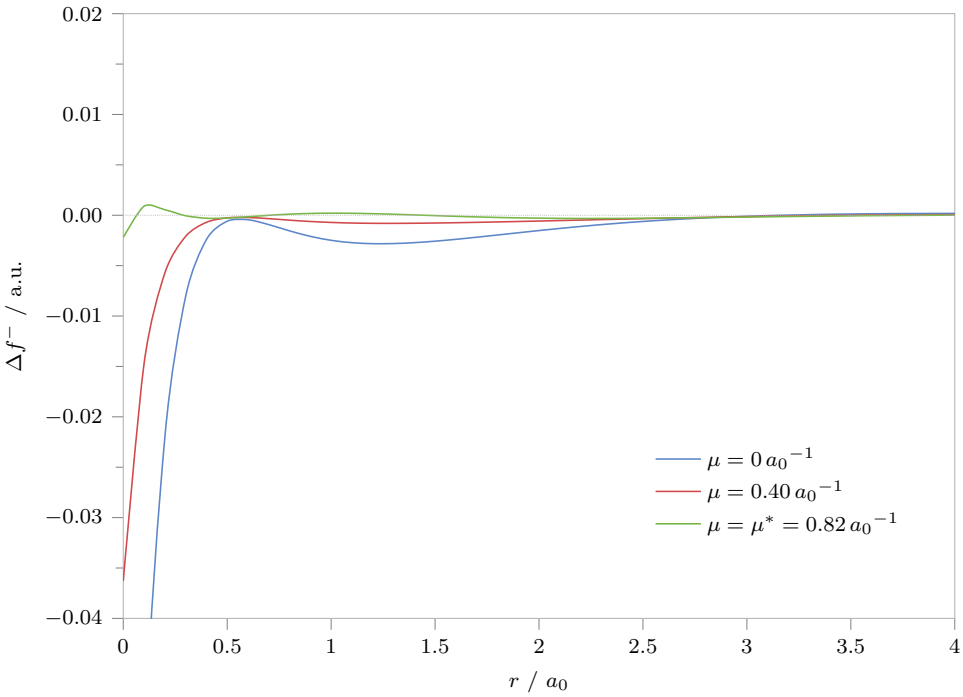

Figure 6: Fukui function differences for the Be atom

4 Acknowledgments

DJT and JDG thank the EPSRC for studentship support. FDP acknowledges the Free University of Brussels (VUB) and the Research Foundation Flanders (FWO) for continuous support.

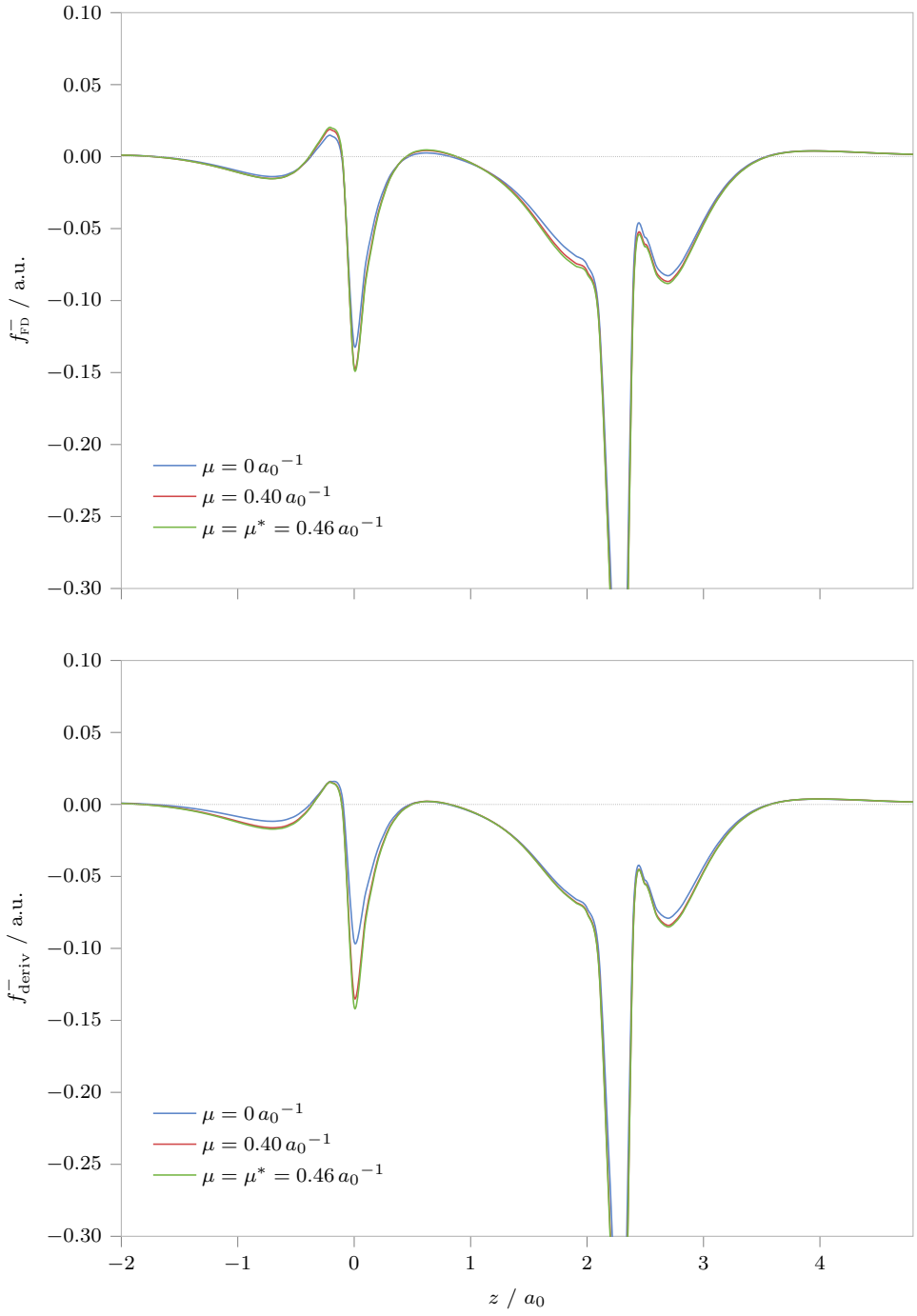

Figure 7: Fukui functions for H_2CO

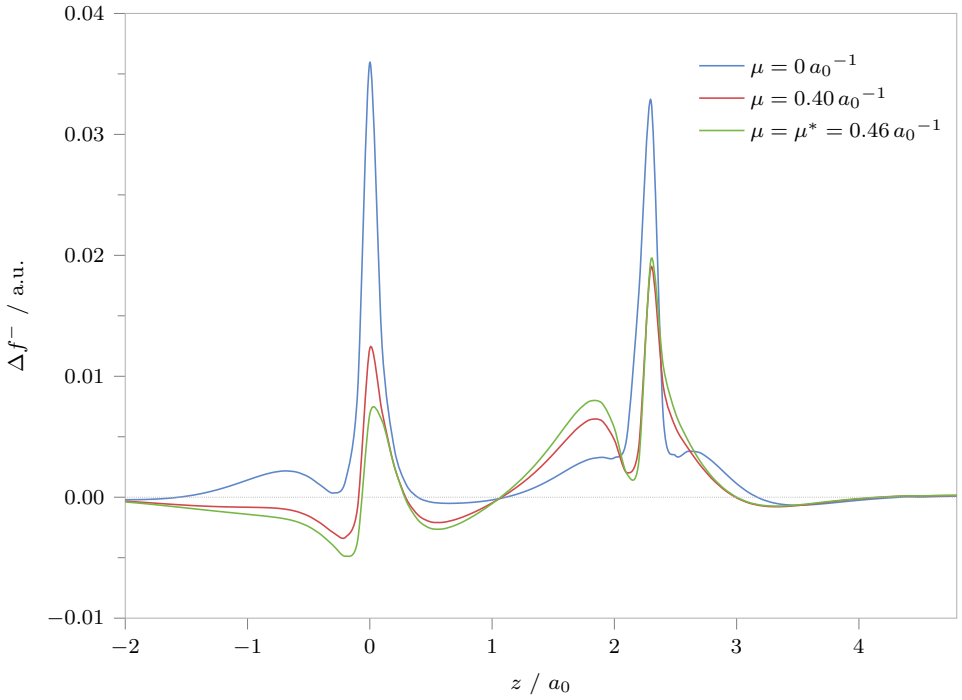

Figure 8: Fukui function differences for H_2CO

References

(1) Gill, P. M. W.; Adamson, R. D.; Pople, J. A. *Mol. Phys.* **1996**, *88*, 1005–1010.

(2) Leininger, T.; Stoll, H.; Werner, H.-J.; Savin, A. *Chem. Phys. Lett.* **1997**, *275*, 151–160.

(3) Iikura, H.; Tsuneda, T.; Yanai, T.; Hirao, K. *J. Chem. Phys.* **2001**, *115*, 3540–3544.

(4) Yanai, T.; Tew, D. P.; Handy, N. C. *Chem. Phys. Lett.* **2004**, *393*, 51–57.

(5) Kohn, W.; Sham, L. J. *Phys. Rev.* **1965**, *140*, A1133–A1138.

(6) Salzner, U.; Baer, R. *J. Chem. Phys.* **2009**, *131*, 231101.

(7) Stein, T.; Eisenberg, H.; Kronik, L.; Baer, R. *Phys. Rev. Lett.* **2010**, *105*, 266802.

(8) Stein, T.; Kronik, L.; Baer, R. *J. Am. Chem. Soc.* **2009**, *131*, 2818–2820.

(9) Stein, T.; Kronik, L.; Baer, R. *J. Chem. Phys.* **2009**, *131*, 244119.

(10) Kuritz, N.; Stein, T.; Baer, R.; Kronik, L. *J. Chem. Theory Comput.* **2011**, *7*, 2408–2415.

(11) Refaely-Abramson, S.; Baer, R.; Kronik, L. *Phys. Rev. B* **2011**, *84*, 075144.

(12) Minami, T.; Nakano, M.; Castet, F. *J. Phys. Chem. Lett.* **2011**, *2*, 1725–1730.

(13) Kronik, L.; Stein, T.; Refaely-Abramson, S.; Baer, R. *J. Chem. Theory Comput.* **2012**, *8*, 1515–1531.

(14) Karolewski, A.; Kronik, L.; Kümmel, S. *J. Chem. Phys.* **2013**, *138*, 204115.

(15) Gledhill, J. D.; Peach, M. J. G.; Tozer, D. J. *J. Chem. Theory Comput.* **2013**, *9*, 4414–4420.

(16) Karolewski, A.; Stein, T.; Baer, R.; Kümmel, S. *J. Chem. Phys.* **2011**, *134*, 151101.

(17) Körzdörfer, T.; Parrish, R. M.; Sears, J. S.; Sherrill, C. D.; Brédas, J.-L. *J. Chem. Phys.* **2012**, *137*, 124305.

(18) Sun, H.; Autschbach, J. *ChemPhysChem* **2013**, *14*, 2450–2461.

(19) Agrawal, P.; Tkatchenko, A.; Kronik, L. *J. Chem. Theory Comput.* **2013**, *9*, 3473–3478.

(20) Garza, A. J.; Osman, O. I.; Asiri, A. M.; Scuseria, G. E. *J. Phys. Chem. B* **2015**, *119*, 1202–1212.

(21) Perdew, J. P.; Parr, R. G.; Levy, M.; Balduz, J. L. *Phys. Rev.* **1982**, *49*, 1691–1694.

(22) Parr, R. G.; Yang, W. T. *J. Am. Chem. Soc.* **1984**, *106*, 4049–4050.

(23) Ayers, P. W.; Levy, M. *Theor. Chem. Acc.* **2000**, *103*, 353–360.

(24) Fukui, K.; Yonezawa, T.; Shingu, H. *J. Chem. Phys.* **1952**, *20*, 722.

(25) Kato, S. *Theor. Chem. Acc.* **2000**, *103*, 219–220.

(26) Fukui, K. *Science* **1982**, *218*, 747–754.

(27) Geerlings, P.; De Proft, F.; Langenaeker, W. *Chem. Rev.* **2003**, *103*, 1793–1874.

(28) Amos, R. D.; Alberts, I. L.; Andrews, J. S.; Cohen, A. J.; Colwell, S. M.; Handy, N. C.; Jayatilaka, D.; Knowles, P. J.; Kobayashi, R.; Laming, G. J.; Lee, A. M.; Maslen, P. E.; Murray, C. W.; Palmieri, P.; Rice, J. E.; Simandiras, E. D.; Stone, A. J.; Su, M.-D.; Tozer, D. J. CADPAC 6.5, The Cambridge Analytic Derivatives Package. 1998.

(29) Frisch, M. J.; Trucks, G. W.; Schlegel, H. B.; Scuseria, G. E.; Robb, M. A.; Cheeseman, J. R.; Scalmani, G.; Barone, V.; Mennucci, B.; Petersson, G. A.; Nakatsuji, H.; Caricato, M.; Li, X.; Hratchian, H. P.; Izmaylov, A. F.; Bloino, J.; Zheng, G.; Sonnenberg, J. L.; Hada, M.; Ehara, M.; Toyota, K.; Fukuda, R.; Hasegawa, J.; Ishida, M.; Nakajima, T.; Honda, Y.; Kitao, O.; Nakai, H.; Vreven, T.; Montgomery Jr., J. A.;

Peralta, J. E.; Ogliaro, F.; Bearpark, M.; Heyd, J. J.; Brothers, E.; Kudin, K. N.; Staroverov, V. N.; Kobayashi, R.; Normand, J.; Raghavachari, K.; Rendell, A.; Burant, J. C.; Iyengar, S. S.; Tomasi, J.; Cossi, M.; Rega, N.; Millam, J. M.; Klene, M.; Knox, J. E.; Cross, J. B.; Bakken, V.; Adamo, C.; Jaramillo, J.; Gomperts, R.; Stratmann, R. E.; Yazyev, O.; Austin, A. J.; Cammi, R.; Pomelli, C.; Ochterski, J. W.; Martin, R. L.; Morokuma, K.; Zakrzewski, V. G.; Voth, G. A.; Salvador, P.; Dannenberg, J. J.; Dapprich, S.; Daniels, A. D.; Farkas, Ö.; Foresman, J. B.; Ortiz, J. V.; Cioslowski, J.; Fox, D. J. Gaussian 09 Revision A.02. 2009.

(30) Cohen, A. J.; Mori-Sánchez, P.; Yang, W. *Phys. Rev. B* **2008**, *77*, 115123.

(31) Perdew, J. P.; Levy, M. *Phys. Rev. Lett.* **1983**, *51*, 1884–1887.

(32) Perdew, J. P. *NATO ASI Ser., Ser. B* **1985**, *123*, 265–308.

(33) Seidl, A.; Görling, A.; Vogl, P.; Majewski, J.; Levy, M. *Phys. Rev. B* **1996**, *53*, 3764–3774.

(34) Becke, A. D. *Phys. Rev. A* **1988**, *38*, 3098–3100.

(35) Becke, A. D. *J. Chem. Phys.* **1993**, *98*, 5648–5652.

(36) Stephens, P. J.; Devlin, F. J.; Chabalowski, C. F.; Frisch, M. J. *J. Phys. Chem.* **1994**, *98*, 11623–11627.

(37) Lee, C.; Yang, W.; Parr, R. G. *Phys. Rev. B* **1988**, *37*, 785–789.

(38) Vosko, S. H.; Wilk, L.; Nusair, M. *Can. J. Phys.* **1980**, *58*, 1200–1211.

(39) Yang, W.; Cohen, A. J.; De Proft, F.; Geerlings, P. *J. Chem. Phys.* **2012**, *136*, 144110.

(40) Senet, P. *J. Chem. Phys.* **1997**, *107*, 2516–2524.

(41) Ayers, P. W. *Theor. Chem. Acc.* **2001**, *106*, 271–279.

(42) Ayers, P. W. *J. Math. Chem.* **2008**, *43*, 285–303.

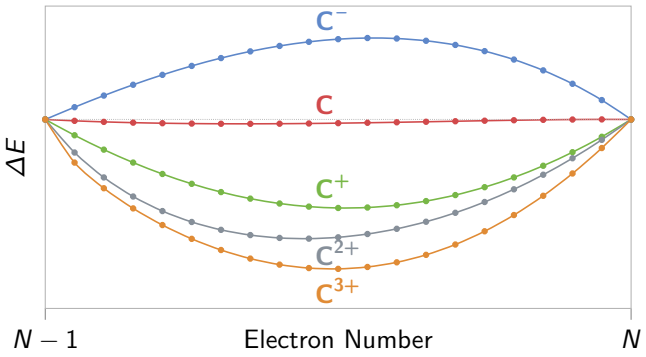

Graphical abstract.